FORSCHUNGSZENTRUM
ROSSENDORF e.V.

FZR

FZR-159
November 1996
Preprint

C.-M. Herbach, H.-G. Ortlepp, P. Gippner, D. V. Kamanin,
Yu. E. Penionzhkevich, G. Renz, K. D. Schilling,
O. V. Strekalovsky, V. G. Tichtchenko, W. Wagner
and the FOBOS-collaboration

Decay Study of Hot Nuclei Below the Multifragmentation Threshold with the FOBOS Detector at Dubna

Invited talk at the
International Research Workshop
"Heavy Ion Physics at Low, Intermediate and Relativistic
Energies using 4π Detectors"
Poiana Brasov, Romania, October 7 - 14, 1996

Forschungszentrum Rossendorf e.V.
Postfach 51 01 19 · D-01314 Dresden
Bundesrepublik Deutschland

Telefon	**(0351) 260 3376**
Telefax	**(0351) 260 3700**
E-Mail	**herbach@fz-rossendorf.de**

DECAY STUDY OF HOT NUCLEI BELOW THE MULTIFRAGMENTATION THRESHOLD WITH THE FOBOS DETECTOR AT DUBNA

C.-M. HERBACH [a] , H.-G. ORTLEPP [a,b] , P. GIPPNER [a] , D.V. KAMANIN [a,b], Yu.E. PENIONZHKEVICH [b], G. RENZ [a] , K.D. SCHILLING [a] , O.V. STREKALOVSKY[b], V.G. TICHTCHENKO [b], W.WAGNER [a,b]
and the FOBOS-collaboration

[a] *Research Center Rossendorf Inc., Institute of Nuclear and Hadronic Physics, Post-Box 510119, D-01314 Dresden, Germany*

[b] *Joint Institute for Nuclear Research, Flerov Laboratory of Nuclear Reactions, 141980 Dubna, Moscow Region, Russia*

The reactions ^{14}N(53AMeV) + ^{197}Au and ^{232}Th have been used to study the three-fold decay of hot heavy compound-like nuclei at excitation energies per nucleon < 3.5 MeV in competition to binary fission. Additionally to the dominant sequential emission of an intermediate mass fragment (IMF) from the target-like nucleus followed fission, a simultaneous decay channel with a large yield of symmetric partition into three heavy fragments was identified by the Coulomb focusing effect. The experimental results can be explained within the frame of a smooth transition from the "neck"-emission to a symmetric ternary fission process.

1 Introduction

The fragment spectrometer FOBOS (refs. [1,2]) was designed to detect charged particles within an extended dynamic energy range and covers - within the angular limits of 20°- 160° with respect to the beam axis - a large portion of the total solid angle of 4π. The detector system has been built at the Flerov Laboratory of Nuclear Reactions of the Joint Institute for Nuclear Research in Dubna, adapted to the basic features of the isocroneous cyclotron U-400M (ref. [3]), namely the set of available projectiles accelerated to bombarding energies of 20 - 100 AMeV (ref. [4]).

The physical programme for the measurements at FOBOS is focused on the study of heavy-ion induced reactions, especially in the low and intermediate region of the Fermi-energy domain. The detector set-up performs a regular covering of the angular range also in the backward hemisphere and makes the FOBOS array well suited, in particular, for investigations of strongly asymmetric projectile-target combinations. For the study of the decay of equilibrated compound-like nuclei, such asymmetric systems have essential advantages with respect to the suppression of the fast reaction channels. In symmetric systems, the yield of fast reaction channels - mainly due to peripheral collisions - increases and results in some serious difficulties for the unambiguous separation

of the reaction types.

The first full-scale high-statistics runs with the complete FOBOS detector configuration were carried out at the beginning of 1996 using thin targets (180-300 $\mu g/cm^2$) of ^{197}Au and ^{232}Th and the ^{14}N beam accelerated to the bombarding energy of 53 AMeV. For the complex fragments, which were detected by the gas-filled detector modules - each of them consisting of a position-sensitive avalanche counter (PSAC) (ref. [5]) mounted at a distance of about 50 cm from the target and a Bragg-ionization chamber (BIC) (ref. [6]) behind them - the individual physical observables mass (A), charge (Z), emission energy (E) and emission direction (θ, ϕ) were deduced from the measured data without use of any introduced correlation between the fragments of the same event. Based on these single fragment parameters, some balances referring to the whole event were calculated in order to define effective selection criteria, e.g. the total fragment mass, the center-of-mass velocity of the decaying system as well as the longitudinal and the transversal components of the total momentum. These balances were used to identify those events with complete detection of all complex fragments produced in the reaction. After this selection, the data considered in the further analysis comprised about 17000 and 32000 events for the ternary decay in the corresponding reactions on ^{197}Au and ^{232}Th, respectively.

The results described in this contribution are dealing with the observation of different decay modes into three complex fragments. The correlations between the emission directions and the relative velocities of the different fragments imply a collinear tripartition similar to the emission of an intermediate mass fragment from the "neck"-zone between the two heavy fission fragments near scission. Moreover, evidence has been found also for ternary fission into fragments with nearly equal masses.

2 Excitation energy of the composite system and its correlation with the total fragment mass and momentum transfer

The decay modes of excited heavy nuclei are determined by the amount of accumulated excitation energy, which is obtained from the incidence energy and transformed into collective energy of the composite system and thermal energy of the nucleons in it. At heavy-ion reactions with bombarding energies > 10 AMeV, the fusion-like process at central collisions decreases in favour of the incomplete fusion reaction (ref. [7]). Due to the broad distributions of the pre-equilibrium particles with regard to the multiplicity, the emission direction and the kinetic energy of the neutrons and the light charged particles (LCP), the compound-like systems survive with different total masses, velocities and excitation energies. For induced excitation energies up to 3.5 MeV per nucleon, binary fission in competition with IMF emission is still one of the dominating channels for the decay of hot heavy nuclei (refs. [8,9]). By selecting the events

with at least two complex fragments, the correlation between the sum of the fragment masses and the total momentum of the decaying system - calculated from the single fragment observables - can be used to estimate the deposited excitation energy within the frame of the Massive-Transfer-Model (ref.[10]). For central collisions of very asymmetric projectile-target combinations, a linear correlation between the portion of the linear momentum transferred from the projectile to the target (LMT) on the one hand and the excitation E* on the other has been well established (ref.[11]). In this manner, we used the velocity of the composite system v_{cm} in relation to the center-of-mass velocity for complete fusion v_{cm}^{max} as a measure for the induced E*. Usually, most of the induced E* is spent by the emission of neutrons and LCP during the de-excitation cascade. In this context, the increase of excitation energy is correlated with a decrease of the number of nucleons which are bound within the fission fragments. Thus, the dependence between the sum of the fragment masses and v_{cm} can be used to prove the deduced E*.

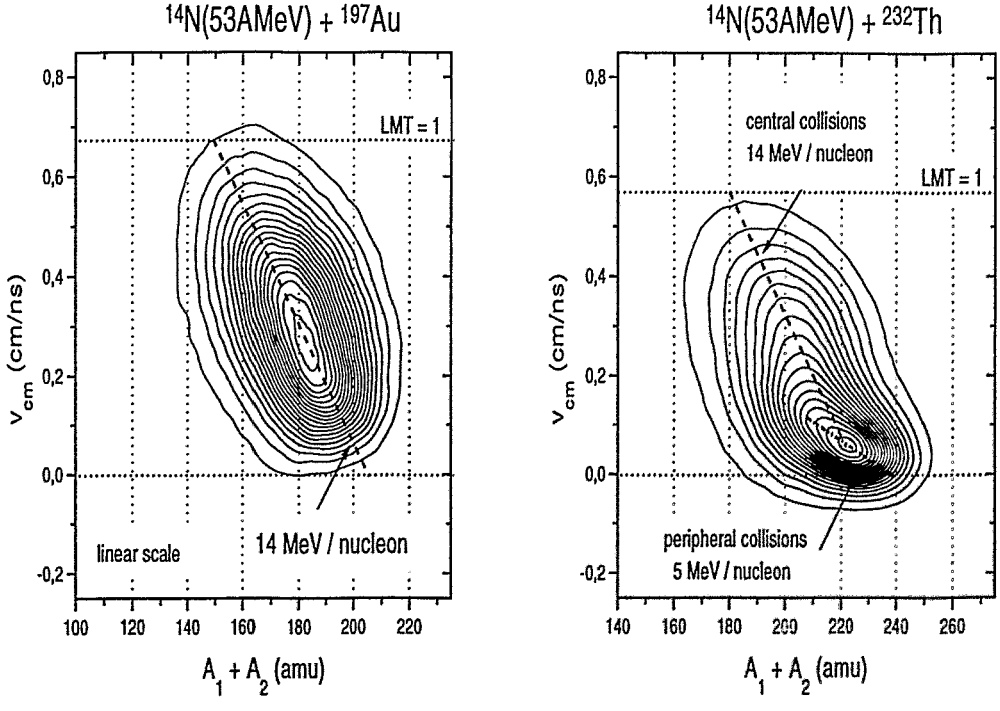

Figure 1: Correlation between total fragment mass and velocity of the composite system

From the correlations in fig. 1, an averaged amount of excitation energy of about 14 MeV to account for the sum of binding and kinetic energy per evaporated nucleon for composite systems produced in central collisions can be deduced. This value is in agreement with the results of ref. [12] for similar systems. However, as indicated by the two fission components for the ^{232}Th target, the correlation changes from central to peripheral collisions. As the fission barrier for ^{197}Au is essentially larger, the fission after peripheral collisions is strongly suppressed. Nevertheless, the excitation energy distributions corresponding to central collisions are in a good agreement for both targets (fig. 2).

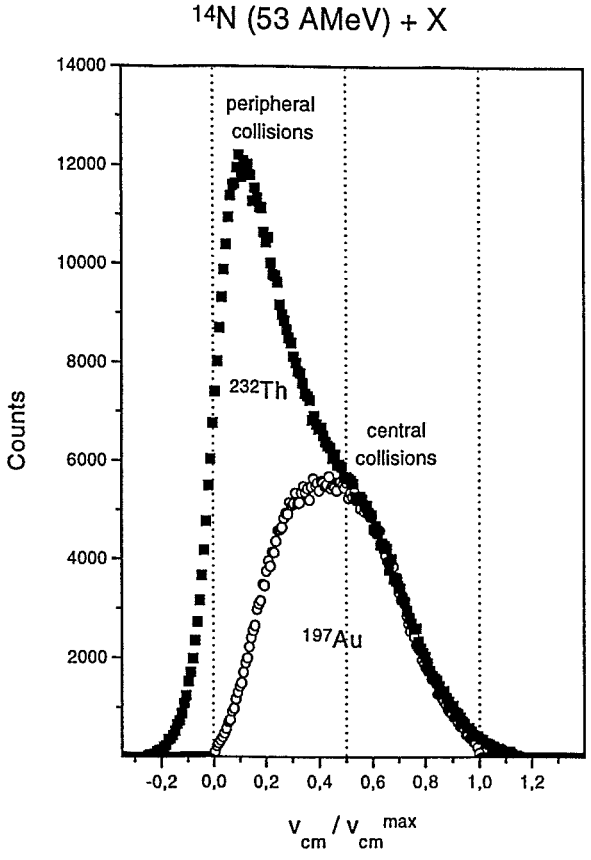

Figure 2: Normalized v_{cm} distribution deduced from binary fission events

3 Ternary fragment decay versus binary fission

In order to select the events of the decay into three complex fragments, the balances were checked in the same way as in the case of binary fission. The fragment mass sum was confined within a moderate range corresponding to the distributions shown in fig. 1, and the transversal component of the total fragment momentum was not allowed to exceed 1200 MeV/c and 1350 MeV/c for the reactions with ^{232}Th and ^{197}Au targets, respectively. These limits correspond to the FWHM of the measured transversal momentum distributions. As a measure of excitation energy, v_{cm} was calculated for the detected fragments. The resulting distributions for FF+FF+IMF-events with Z_{IMF} = 3–8 are compared with the spectra from binary fission (fig. 3). Evidently, the three-fold events are mainly produced in central collisions, and even for the

^{232}Th target the peripheral reaction channel has no essential influence on the production of ternary events.

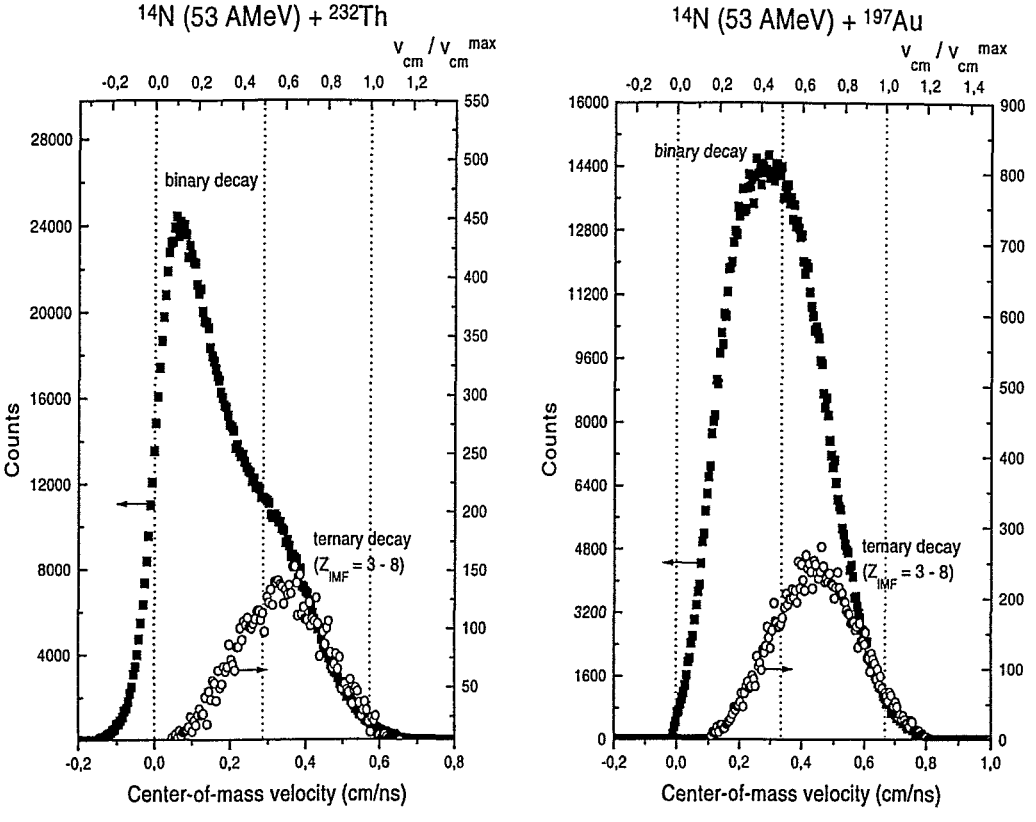

Figure 3: Comparision of v_{cm} distributions for binary and ternary decay

The yield ratio of the ternary events with respect to binary fission is shown in fig. 4 for different values of the excitation energy per nucleon (deduced from v_{cm}). By calculating this ratio, an averaged geometrical efficiency for the IMF-detection was taken into account. The results of previous measurements at FOBOS (refs. [13,14]), which were performed for similar systems but at lower bombarding energies, are included in fig. 4 for comparison. For excitation energies lower than 1.5 MeV/nucleon, the IMF-yields are reduced by a factor of 10 in comparison to data not related to fission fragments (ref. [15]). This indicates that for lower E* the fission after IMF-emission is strongly suppressed. With increasing excitation energy, the influence of the IMF emission on fission at the end of the de-excitation process becomes smaller. A detailed analysis of fission in competition to heavy-residue production under the influence of IMF-emission is the subject of further investigations.

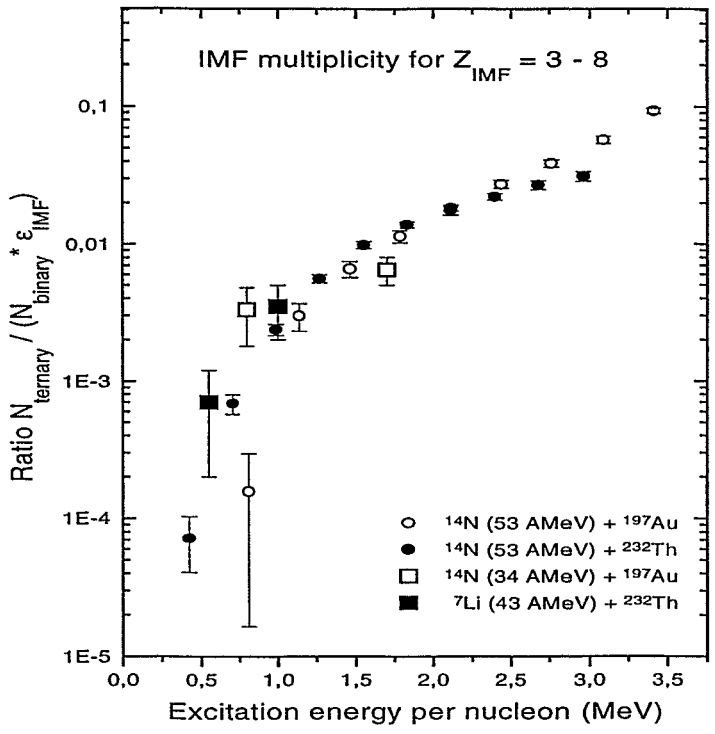

Figure 4: Ratio of ternary events ($N_{ternary}$) to binary fission (N_{binary}) as a function of excitation energy per nucleon of the composite system

4 Angular correlations and relative fragment velocities for ternary events

In the following, we cancel our restriction with respect to the IMF charge as defined before and consider all three-fold events in our analysis including also alpha-particles and charges $Z > 8$ for the lightest of the three detected fragments. However, the events must fulfil the same global requirements as described in chapter 3.

An outstanding feature of the gas-filled modules of the FOBOS-detector is the accuracy in the measurement of the emission direction with an experimental uncertainty of about 0.2°. Combined with the time-of-flight and the residual energy measurements - the low-energy detection threshold amounts to 0.6 AMeV - FOBOS is especially suited for the sensitive analysis of angular correlations and relative fragment velocities even for symmetric tripartitions.

The basic observables of the analysis discussed in this chapter are illustrated

in fig. 5 within the center-of-mass system of the detected fragments. The two heaviest particles are labelled as fission fragments, and a reduced composite system C' is defined by this fragment pair.

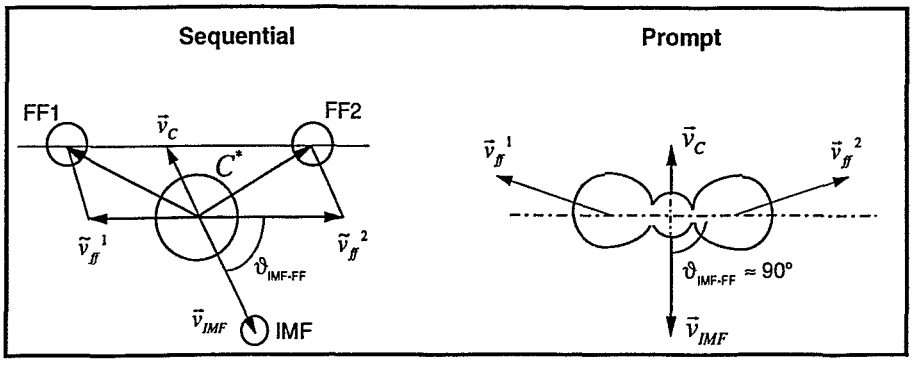

Figure 5: Definition of ϑ_{IMF-FF} as the angle of IMF emission direction with respect to the fission axis and the relative velocity v_{IMF-FF} between the IMF and the residual system

For the analysis of the angular correlation, a transformation has been carried out into the rest frame of the composite nucleus C'. Consequently, per definition, the trajectory of the fission fragments includes the constant angle of 180° and the fission axis is defined unambiguously. For the sequential decay, consisting in the emission of the lightest particle (IMF) from the composite system (C'+IMF) in the first step and followed by fission as the second reaction step, the distribution between the IMF emission direction and the fission axis is expected to be isotropical. The situation changes, when the decay occurs simultaneously: The IMF is focused by the Coulomb forces of the two fission fragments and its emission is favoured perpendicularly to the fission axis.

Another hint on the difference between the two modes is the relative velocity between the reduced composite system C' and the IMF. The sequential decay is correlated with relative velocities corresponding to the Coulomb repulsion of the IMF during the evaporation from a compact target-like nucleus. In contrast to this, the relative velocity of the IMF emitted from the strong deformed system near scission as shown in the fig. 5 should be significantly reduced.

Such an observation has already been reviewed for IMF with $Z < 8$ (ref.[16]). And indeed, our experimental data shown in fig. 6 confirm the existence of a simultaneous decay channel with Coulomb focusing, which delivers IMF within the relative velocity range of 1.5-2.3 cm/ns. These events are clearly separated from the dominant yield of IMF isotropically emitted with relative velocities

of 2.5-3.5 cm/ns. Additionally, two further isotropic decay channels are visible: A significant yield is observed both at very large relative velocities of 3.8-5.0 cm/ns and at extremely low relative velocities below 2.0 cm/ns down to the threshold at 0.9 cm/ns.

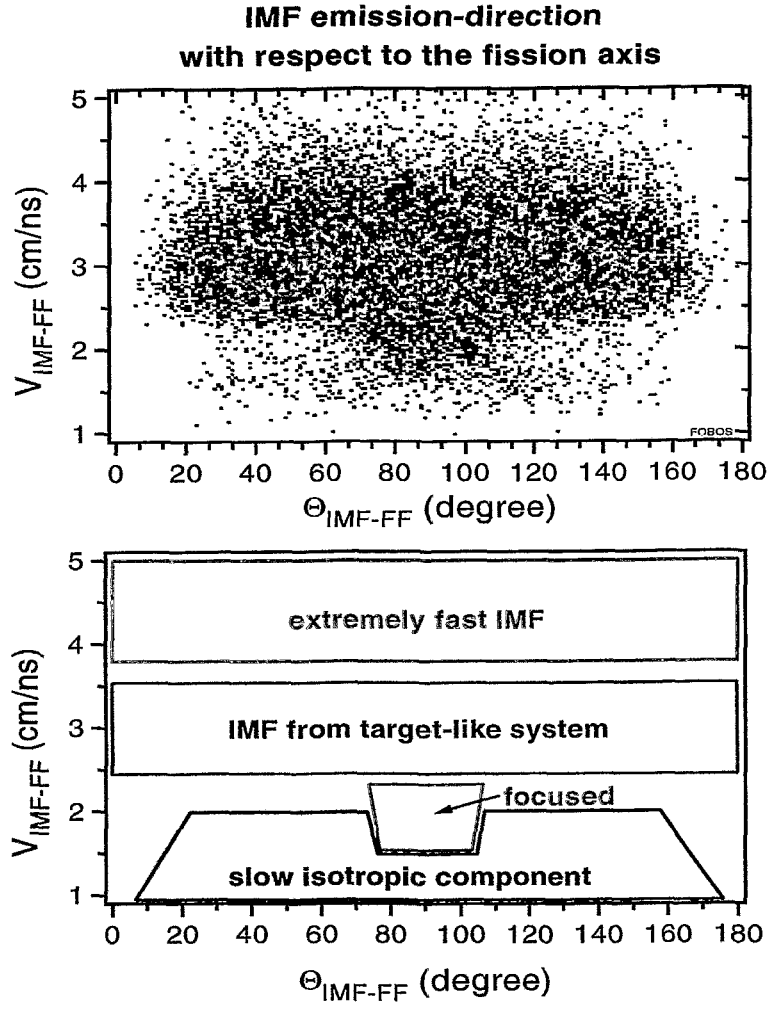

Figure 6: Identified modes of three-fold decay (for details see text)

In order to prove the Coulomb focusing effect, the angular distributions of the events with relative velocities below 2.3 cm/ns were analyzed considering three different mass-asymmetry ratios of the associated fission fragments.

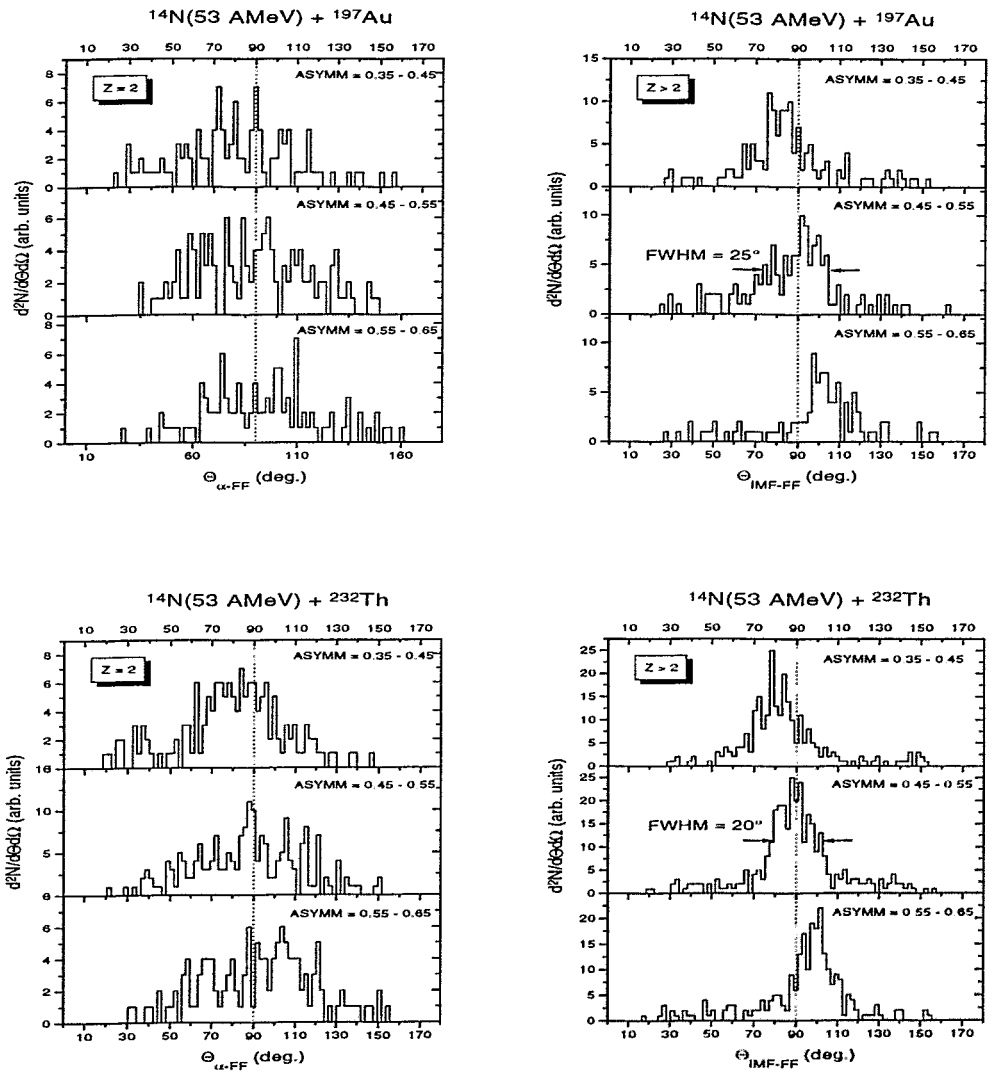

Figure 7: Angular distributions $\Theta_{\alpha-FF}$ and Θ_{IMF-FF} for the lightest fragments with $v_{IMF-FF} < 2.3$ cm/ns as a function of the mass-asymmetry of the two heaviest fragments

In the upper parts of the pictures in fig. 7, the largest fragment is emitted in positive direction along the x-axis, the parts in the middle show the distribution for symmetric fission and the lower parts refer to the opposite fragment mass asymmetry as used for the event selection in the upper parts. The pictures in fig. 7 differ in the two targets ^{197}Au and ^{232}Th and in the charge of the lightest fragment Z=2 and Z>2, respectively. For symmetric fission, the mean value of the peak in the angular distribution is very close to 90°. This peak shifts for about 10° into the direction of the lighter fission fragment in the case of more asymmetric fission. Corresponding with the different Coulomb forces,

the focusing effect increases with the charge of the lightest fragment and is stronger for the reaction with the ^{232}Th target than for the ^{197}Au target.

5 Excitation energy dependence of the tripartition and charge distribution of the lightest fragments

The four different modes of three-fold decay are classified by gates within the Θ_{IMF-FF} - v_{IMF-FF}- matrix as displayed in fig. 6. The corresponding yield ratios between ternary and binary events are shown in fig. 8 for the different groups of three-fold events in dependence on the primary induced E*. For this analysis, the alpha particles as lightest third particle are excluded.

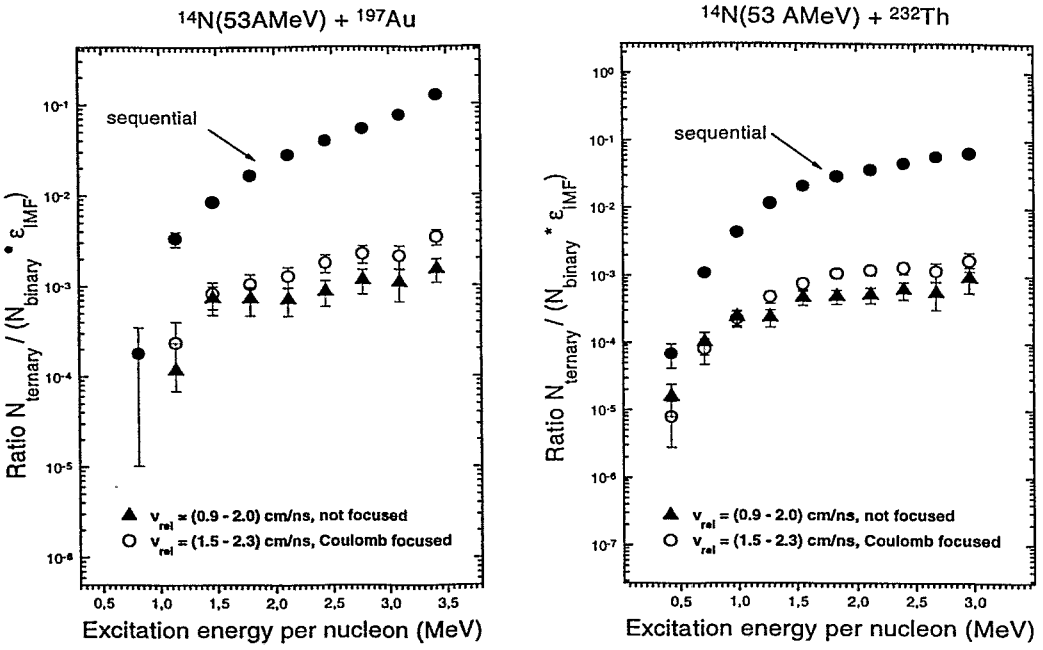

Figure 8: Relative yields of ternary decay modes in dependence on the excitation energy

It is evident that the dependence on the excitation energy above the threshold at about 200 MeV for the both components with lower relative velocities < 2.3 cm/ns is less than for the dominant yield of sequential decay. As known from binary fission (ref.[17]), such a behaviour can be expected for a slow process. Since the evaporation of neutrons, LCP and IMF from the composite system at the beginning of the de-excitation cascade becomes faster with the increase of the primary induced excitation energy, the difference between the remaining excitation energies is reduced successively and can be neglected after a sufficient large period of the de-excitation cascade.

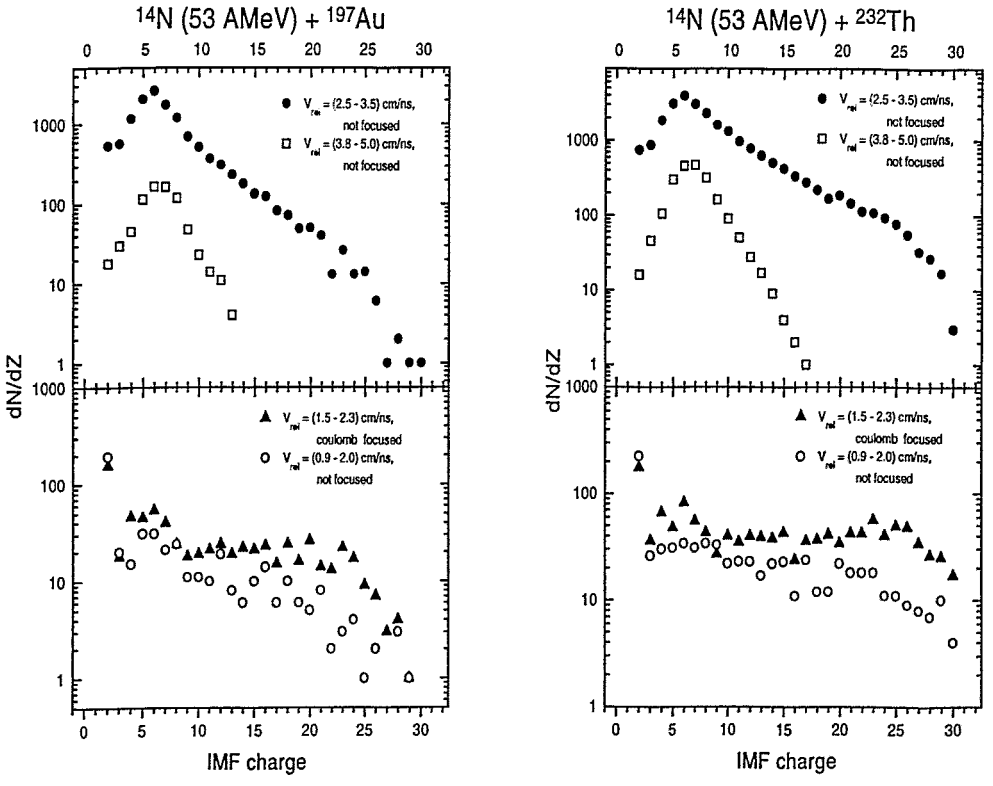

Figure 9: Charge distributions of the different ternary decay modes

Another surprising result is the charge distribution shown in fig. 9 for the different classes of three-fold-events. One should mention that for $Z < 6$ the detection efficiency of the PSAC may be less than 100%. Nevertheless, the most interesting result is the large amount of heavy fragments as third particle for both modes referring to the lower relative velocities. In particular for the focused component, the yield between $Z = 10$ and $Z = 20$ is nearly constant and seems to increase for charges corresponding to a decay into three fragments with similar masses.

6 Evidence of collinear tripartition into symmetric mass splits

In this chapter, we want to find out the type of the configuration, which corresponds with the simultaneous Coulomb focused decay. For this aim, we used a cut within the Dalitz-plot of the three fragments in order to select the events with three fragments of similar masses.

These events are sorted into the matrix of fig. 10, which displays the correlation between the already defined relative velocity v_{IMF-FF} and the

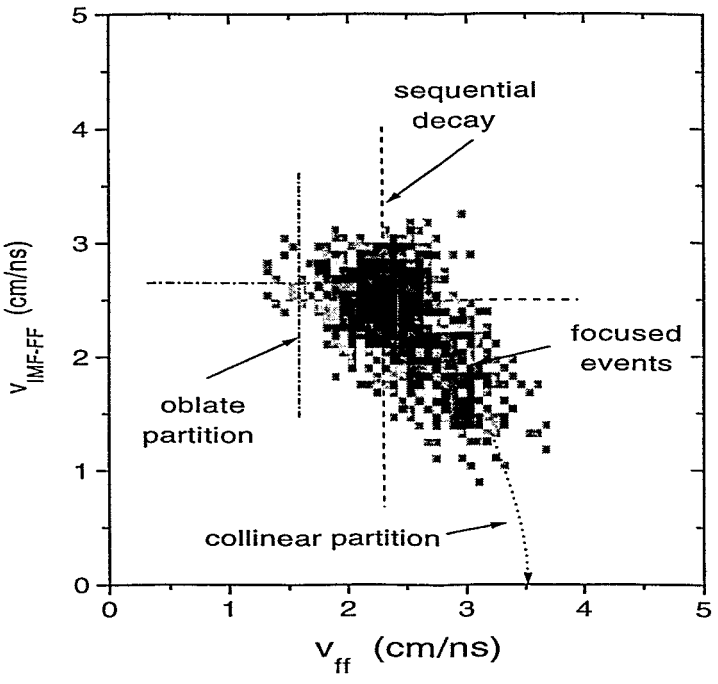

Figure 10: Relative velocity v_{IMF-FF} between the lightest fragment and the residual system versus relative velocity v_{ff} between the two heaviest fragments, observed for ternary decay into fragments of nearly equal masses

relative velocity v_{ff} of the two heaviest fragments. Assuming the decay into three equal fragments, we calculated this observables using the systematics of *Viola* (ref. [18]) for the tripartition of the nucleus of A=180 and Z=81, which corresponds to a typical composite system for the reaction on ^{197}Au. In the case of sequential decay, the calculation results in 2.3 cm/ns and 2.5 cm/ns for v_{ff} and v_{IMF-FF}, respectively. Considering a prompt decay of an oblate configuration, where the three fragments are arranged with relative angles of 120° at the corner of a triangle with equal sides, the corresponding values are 1.6 cm/ns and 2.7 cm/ns, respectively. The largest value of v_{ff} is achieved for the prompt decay of a collinear configuration and amounts to 3.5 cm/ns. In this case, the theoretical value for v_{IMF-FF} goes to zero. The comparison of our experimental data with these simple estimations indicates that both values measured for the Coulomb focused component are in a good agreement with the simultaneous tripartition from a nearly collinear configuration and differ significantly from the oblate partition.

7 Summary

The three-fold decay of heavy hot nuclei was analyzed for the reactions ^{14}N(53AMeV) + ^{197}Au and ^{232}Th by using the fragment spectrometer FOBOS. Since the results for both targets are very similar, the decaying composite systems were mostly produced in central collisions and the influence of the peripheral entrance channel can be neglected. The dominant three-fold decay mode is the sequential emission of an IMF from a target-like nucleus followed fission. Additionally, a simultaneous decay channel was identified from the observed Coulomb focusing effect of the lightest particle. The charge distribution of the lightest fragment group in this decay mode covers a large range up to the symmetric tripartition with a nearly constant yield for $Z > 10$. The weaker dependence of the yield on the induced E^* is in agreement with the description of this decay as a slow fission-like process. The relative velocities between the three fragments correspond with a collinear configuration of the tripartition. Based on these observations, we propose to interpret the measured data within the picture of a smooth transition from the "neck"-emission to a symmetric ternary fission process which has been predicted more than 20 years ago by *Diehl and Greiner* (ref. [19]) within the framework of the liquid drop model. A similar mode of tripartition, which is characterized by extremely low relative velocities but isotropic emission of the third particle with respect to the fission axis, is interpreted as ternary fission accompanied with a delayed neck rupture.

Acknowledgments

The authors thank all the members of the FOBOS collaboration for their contributions by building up the detector device and for technical assistance at the measurements. In particular, we want to thank Prof. Yu.Ts. Oganessian and Prof. E. Grosse for their support of the present work. We are indebted to the staff of the U-400 cyclotron for the outstanding cooperation during the experiments, especially to B.N. Gikal, G.G. Gulbekian and V.B. Kuttner. The work presented was supported by the Bundesministerium fuer Bildung und Forschung under the contract 06 DR 671

References

1. H.-G. Ortlepp *et al.*, Proc. Int. Conf. on New Nuclear Physics with Advanced Techniques, Ierapetra, Greece, 1991, World Scientific, Singapore, 1992, p. 302
2. H.-G. Ortlepp *et al.*, Proc. Int. School-Seminar on Heavy Ion Physics, Dubna, Russia, 1993, JINR E7-93-247, Dubna, 1993, vol.2, p. 466
3. G.N. Flerov *et al.*, Report JINR 9-84-55, Dubna, Russia, 1984

4. G.G.Gulbekian and V.B. Kuttner, Proc. of the FOBOS Workshop '94, Cracow, Poland, 1994, FZR-65, Rossendorf, 1995, p. 25
5. W. Seidel *et al.*, *Nucl. Instrum. Methods* A **273**, 536 (1988)
6. H.-G. Ortlepp and A. Romaquera, *Nucl. Instrum. Methods* A **267**, 500 (1989)
7. V.E. Viola,Jr. *et al.*, *Phys. Rev.* C **26**, 178 (1982)
8. E. Schwinn *et al.*, *Nucl. Phys.* A **568**, 169 (1994)
9. A.A. Sonzogni *et al.*, *Phys. Rev.* C **53**, 243 (1996)
10. D. Guerreau, Int. School on Nucl. Phys. "Nuclear Matter and Heavy Ion Collisions", Les Houches, France, 1989, Report GANIL P 89-07, Caen, 1989
11. G. Klotz-Engmann *et al.*, *Nucl. Phys.* A **499**, 392 (1989)
12. E.C. Pollacco *et al.*, *Phys. Lett.* B **146**, 29 (1984)
13. A.A. Aleksandrov *et al.*, *Nucl. Phys.* A **583**, 465c (1994)
14. H.-G. Ortlepp *et al.*, XV. Nucl. Phys. Divisional Conf. of the European Physical Society, St. Petersburg, Russia, 1995, in: "Low Energy Nuclear Dynamics", World Scientific, Singapore, 1995, p.231
15. A. Sokolov *et al.*, *Nucl. Phys.* A **562**, 273 (1993)
16. D.E. Fields *et al.*, *Phys. Rev. Lett.* **69**, 3713 (1992)
17. D. Hilscher and H. Rossner, *Ann. Phys. Fr.* **22**, 471 (1992)
18. V.E. Viola *et al.*, *Phys. Rev.* C **31**, 1550 (1985)
19. H. Diehl and W. Greiner, *Phys. Lett.* B **45**, 35 (1973)